ACS Catalysis

Research Article

pubs.acs.org/acscatalysis

Well-Defined Iron Catalysts for the Acceptorless Reversible Dehydrogenation-Hydrogenation of Alcohols and Ketones

Sumit Chakraborty,[†,⊥] Paraskevi O. Lagaditis,[‡,⊥] Moritz Förster,[§] Elizabeth A. Bielinski,[∥] Nilay Hazari,[∥] Max C. Holthausen,[§] William D. Jones,*[,†] and Sven Schneider*[,‡]

[†]Department of Chemistry, University of Rochester, Rochester, New York 14627, United States

[‡]Institut für Anorganische Chemie, Georg-August-Universität, Tammannstraße 4, 37077 Göttingen, Germany

[§]Insitut für Anorganische und Analytische Chemie, Goethe-Universität, Max-von-Laue-Strasse 7, 60438 Frankfurt am Main, Germany

[∥]Department of Chemistry, Yale University, P.O. Box 208107, New Haven, Connecticut 06520, United States

Supporting Information

ABSTRACT: Acceptorless dehydrogenation of alcohols, an important organic transformation, was accomplished with well-defined and inexpensive iron-based catalysts supported by a cooperating PNP pincer ligand. Benzylic and aliphatic secondary alcohols were dehydrogenated to the corresponding ketones in good isolated yields upon release of dihydrogen. Primary alcohols were dehydrogenated to esters and lactones, respectively. Mixed primary/secondary diols were oxidized at the secondary alcohol moiety with good chemoselectivity. The mechanism of the reaction was investigated using both experiment and DFT calculations, and the crucial role of metal−ligand cooperativity in the reaction was elucidated. The iron complexes are also excellent catalysts for the hydrogenation of challenging ketone substrates at ambient temperature under mild H_2 pressure, the reverse of secondary alcohol dehydrogenation.

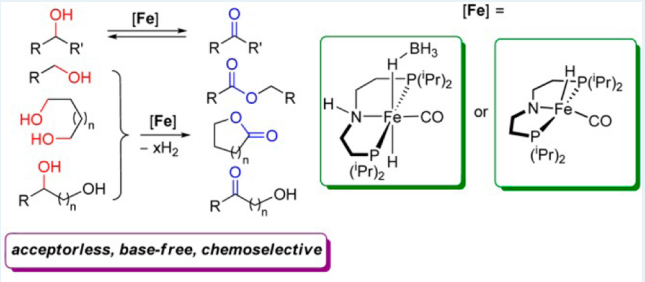

KEYWORDS: *iron, catalysis, acceptorless dehydrogenation, hydrogenation, metal−ligand cooperativity*

INTRODUCTION

Catalytic acceptorless alcohol dehydrogenation (AAD) is a convenient, atom-economical approach for alcohol oxidation without the need for an oxidant.[1] The reaction is also highly relevant to the field of organic-hydrogen-storage-materials as it provides a unique opportunity to release H_2 from sustainable sources, such as biomass-derived alcohols and carbohydrates under mild conditions.[2] Furthermore, reactive carbonyl compounds generated from AAD can be transformed into other useful organic materials such as imines and amides.[3] From a thermodynamic point of view, alcohol dehydrogenation is generally an uphill process (i.e., endothermic) at room temperature;[4] however, the release of H_2 gas has a favorable positive entropic contribution and the de/hydrogenation equilibrium can be driven by removal of H_2.[5]

Despite the significance of this reaction, homogeneous catalysts for AAD protocols mostly employ precious and heavy metals such as Ru,[6] Rh,[7] Ir,[6o,8] and Os.[9] In comparison, the same reaction with catalysts that utilize nonprecious, earth-abundant metals is much less developed. Hanson and co-workers reported a cobalt catalyst (**1**) for AAD which is stabilized by a bis(phosphino)amine (PNP) ligand (Scheme 1).[10] Several secondary aromatic and aliphatic alcohols were dehydrogenated under oxidant-free conditions. Labeling studies indicated an initial reversible alcohol dehydrogenation step involving a cobalt hydride intermediate. Moreover, a catalytic cycle consisting of $Co^{I/III}$ intermediates was proposed, and the importance of metal−ligand cooperativity was highlighted.[11] In the case of a primary alcohol, **1** was found to be much less effective. Nevertheless, dehydrogenation of primary alcohols was achieved in the presence of primary amines, and the corresponding imines were isolated from the Schiff-base reaction.[10] Noticeably, for the dehydrogenative coupling of primary alcohols and amines, comparable catalytic activities to previously reported Ru-based catalysts were reported (1 mol % catalyst **1**), whereas AAD required much higher catalyst loadings (5 mol %).

Scheme 1. Cobalt-Catalyzed Acceptorless Dehydrogenation of Alcohols and Dehydrogenative Coupling of Primary Alcohols and Amines

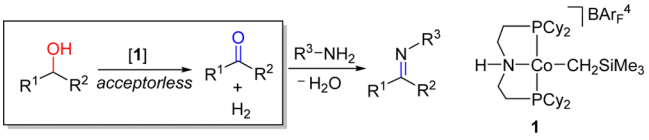

Received: July 7, 2014
Revised: September 24, 2014
Published: September 25, 2014

   dx.doi.org/10.1021/cs5009656 | ACS Catal. 2014, 4, 3994−4003

Most recently, several groups independently reported the synthesis of iron complexes (**2**, **3**, **4**, and related species) supported by chelating PNP ligands and their utilization in de/hydrogenation catalysis (Scheme 2).[12−17] Initially, the Beller

Scheme 2. Catalytic Applications of PNP Supported Iron Complexes

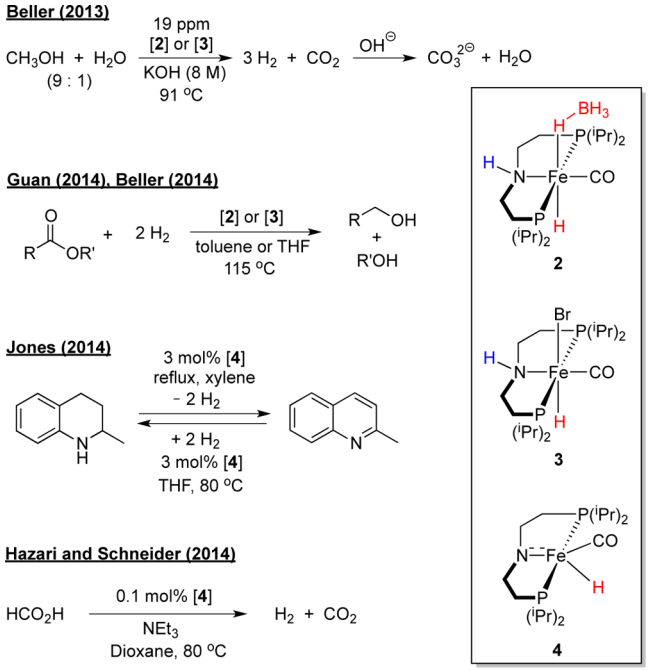

group used complex **2** for catalytic H_2 production from methanol in the presence of KOH.[12] The reaction proceeds at a remarkably low catalyst loading (ppm level), and the high catalyst thermal stability (>90 °C) is noteworthy. Guan[15] and Beller[16] subsequently utilized precatalysts **2** and **3** for ester hydrogenation, and Jones[17] reported the reversible de/hydrogenation of N-heterocycles with these complexes. The hydride amido species **4**, which had been previously proposed by Beller as a crucial catalytically active intermediate, was also isolated and could be directly used as catalyst for this reaction.[17] At the same time, Hazari and Schneider established that **4** can be used as a catalyst for formic acid dehydrogenation and described the equilibrium of **4** with the *cis*- and *trans*-dihydrides $[Fe(H)_2CO\{HN(CH_2CH_2PiPr_2)_2\}]$ (**5a**/**b**) upon H_2 addition/elimination.[14] As a joined, ongoing effort to develop base metal catalysts for de/hydrogenation, we here report new protocols for AAD of secondary and primary alcohols with the well-defined iron catalysts **2**−**4**, as had been predicted in a theoretical study.[18] Furthermore, we show that these species are also active for the reverse ketone hydrogenation of challenging substrates and describe initial experimental and computational mechanistic studies.

RESULTS AND DISCUSSION

We first studied AAD of 1-phenylethanol with precatalysts **2** and **3** under a variety of catalytic conditions (Table 1). The best results were obtained in refluxing toluene under a slow, steady N_2 flow (entry 3). Under these conditions with 1 mol % catalyst (**2**) loading 1-phenylethanol was quantitatively converted to acetophenone within 24 h as determined by ^1H NMR spectroscopy. The identity of the liberated gas was

Table 1. Acceptorless Dehydrogenation of 1-Phenylethanol Using Iron Pincer Complexes (2 and 3) as the Precatalysts

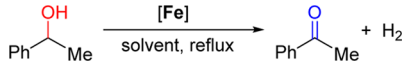

entry	catalyst (loading)	solvent	additive	time (h)	NMR conv. (%)
1	**2** (3 mol %)	THF		24	87
2	**2** (3 mol %)	toluene		24	100
3	**2** (1 mol %)	toluene		24	100
4[a]	**3** (3 mol %)	THF	KO^{t}Bu	24	79
5	**3** (3 mol %)	THF		24	<5
6		toluene		24	0

[a]10 mol % of KO^{t}Bu was used with respect to catalyst **3**.

examined by introducing the gas through a thick cannula into a separate reaction vessel containing cyclooctene, 4 mol % $RhCl(PPh_3)_3$, and 3 mL of THF at 60 °C.[19] Analysis of these reaction products by GC-MS revealed clean formation of cyclooctane, confirming the release of H_2 upon AAD with precatalyst **2**. Further confirmation of H_2 formation is provided by GC headspace gas analysis (see the Supporting Information). Complex **3** was also found to be an AAD precatalyst in the presence of KO^{t}Bu, although lower conversions were obtained after the same time (entry 4). Almost no conversion was observed with complex **3** in the absence of base (entry 5), and no reaction occurred in the absence of any iron catalyst (entry 6).

The substrate scope of AAD with precatalyst **2** was investigated (Scheme 3). Secondary benzylic alcohols (**A**−**I**, **K**, **L**) are dehydrogenated to the corresponding acetophenone derivatives in good isolated yields (65−92%). The reaction is tolerant to a variety of functional groups such as -OMe, -Me, and -NO_2 as well as halides (F, Cl, Br, and I). *ortho*-Methylated substrate **D** exhibits slower reaction rates than *para* and *meta* substituted substrates **C** and **E**. Importantly, for alcohols with electron-withdrawing substituents (**F**−**I**), the catalyst loading can be further lowered to 0.1 mol % (TON = 10^3), albeit with longer reaction times. In addition to aromatic substrates, the aliphatic secondary alcohol cyclohexanol (**J**) was successfully dehydrogenated to give cyclohexanone. A substrate with an ester functional group (**K**) was also tolerated under these conditions.

Both homogeneous and heterogeneous catalysis was recently proposed for (transfer-)hydrogenation with related iron precatalysts, and distinguishing mechanisms can be challenging.[20] All (de)hydrogenation reactions reported here remained as transparent colored solutions throughout the reaction. Beller previously reported that MeOH reforming with **2**/KOH was unaffected by substoichiometric amounts of PMe_3 and hence indicative of homogeneous catalysis. Likewise, in our case the Hg-poisoning test did not affect the reaction; however, mercury does not always inhibit iron nanoparticle catalysts.[20e,f] Therefore, kinetic indications are generally more significant. Dehydrogenation of **F** with **4** was followed over time (see the Supporting Information), and no induction period was observed as, e.g., for Morris' heterogeneous iron transfer catalyst.[20e,f] Furthermore, in the dehydrogenation of **A** (catalyst **2**) the addition of a second batch after full conversion resulted in 53% conversion within the same reaction time. This result suggests that decomposition of **2** does not form a catalytically more active species (see below).

dx.doi.org/10.1021/cs5009656 | ACS Catal. 2014, 4, 3994−4003

Scheme 3. Iron-Catalyzed Acceptorless Dehydrogenation of Alcohols using Precatalyst 2

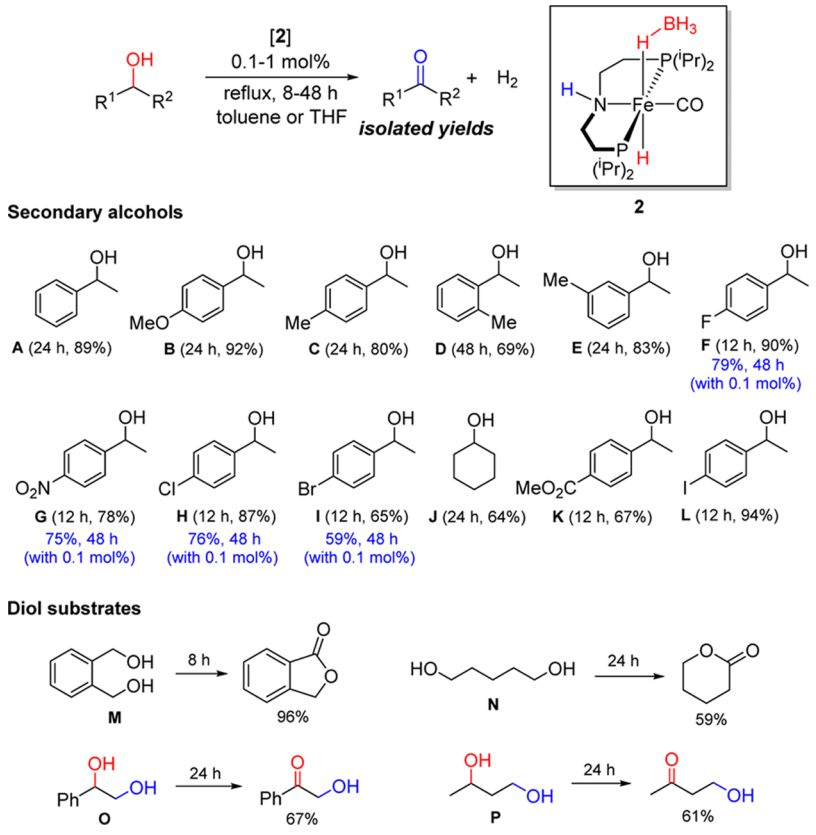

Besides secondary alcohols, primary alcohols and diols were also examined. AAD of benzyl alcohol with precatalyst **2** gives full conversion after 8 h in refluxing toluene and benzyl benzoate was isolated as the sole product from this reaction (eq 1).

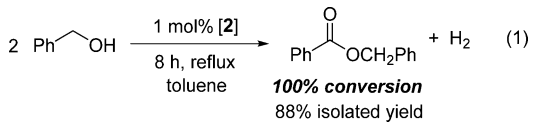

Product formation of the formal dehydrogenative Tishchenko reaction presumably results from addition of substrate to intermediate benzaldehyde and subsequent dehydrogenation of the hemiacetal (see below). Accordingly, intramolecular, dehydrogenative condensation of primary diols, such as 1,2-benzenedimethanol (**M**) and 1,5-pentanediol (**N**), using precatalyst **2**, readily produces the corresponding lactones, phthalide, and δ-valerolactone. Several groups have previously reported homogeneous catalysts for the base-free transfer-dehydrogenation of diols to lactones in the presence of a hydrogen acceptor such as acetone.[21] However, reports related to base-free acceptorless conversion are extremely rare,[22] and the use of a first-row transition metal-based homogeneous catalyst was only recently described for the first time.[23,24]

The chemoselectivity of AAD was explored using two substrates with both primary and secondary alcohol functional groups. Complex **2** selectively dehydrogenates the secondary alcohol moiety in 1-phenyl-1,2-ethanediol (**O**), leaving the primary alcohol unaffected. While the methine C−H bond in **O** is weakened in the presence of the adjacent phenyl group replacement of the phenyl group with a methyl substituent (**P**) also results in exclusive secondary alcohol oxidation (4-hydroxy-2-butanone). Precedence for such high secondary over primary alcohol chemoselectivity in homogeneous alcohol oxidation has been observed for only a few precious metal-based systems.[6n,25]

A plausible homogeneous mechanism for the iron-catalyzed alcohol dehydrogenation is outlined in Scheme 4. Based on our

Scheme 4. Proposed Catalytic Cycle for the Dehydrogenation of Alcohols

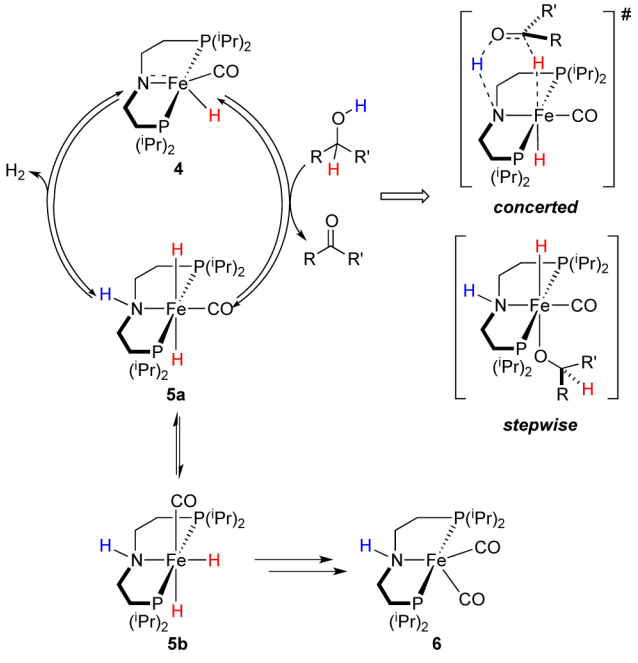

dx.doi.org/10.1021/cs5009656 | ACS Catal. 2014, 4, 3994−4003

current understanding of the dehydrogenation of N-heterocycles[17] and formic acid[14] we propose that complex **4** is directly on the catalytic cycle. Previously, it was established that **4** reversibly adds H_2 to give mainly *trans*-dihydride complex **5a** and smaller amounts of *cis*-dihydride **5b**, which is in equilibrium with **5a** according to EXSY NMR experiments.[14] Minor quantities of free $N(CH_2CH_2P^iPr_2)_2$ and iron(0) complex $[Fe(CO)_2\{HN(CH_2CH_2P^iPr_2)_2\}]$ (**6**)[13] are also observed. The relevance of **4** within the catalytic cycle of AAD is supported by a stoichiometric control reaction of **4** with 2 equiv of 1-butanol at room temperature. Slow, selective substrate conversion to *n*-butyl-butanoate is accompanied by formation of the same iron products (**5a**, **5b**, **6**) and free ligand as determined by ^{31}P NMR spectroscopy, without detection of other intermediates. Hydrogen transfer from the substrate to **4** is conceivable either by a concerted pathway or stepwise through an alkoxide intermediate (Scheme 4), which remains at this point unresolved on experimental grounds. However, our computational results indicate low barriers for a concerted mechanism (see below). Comparison of the stoichiometric reactions of **4** with H_2 and 1-butanol, respectively, indicate considerably faster catalyst degradation to iron(0) and free ligand with alcohol as hydrogen source. This observation suggests that formation of inactive **6** might be initiated by H_2 reductive elimination from **5b** at low H_2 concentrations. In contrast, H_2 elimination from **5a** to amide **4** was shown under vacuum[14,17] and closes the cycle in Scheme 4.

This mechanistic proposal suggests that complex **4** should be an active catalyst for AAD under base free conditions. Accordingly, 1-phenylethanol is selectively converted to acetophenone in boiling toluene with 1 mol % **4** as the catalyst (eq 2). Likewise, selective, dehydrogenation of several primary

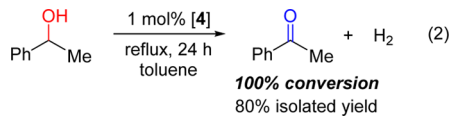

(2)

alcohols to the respective esters is catalyzed by **4** with catalyst loadings as low as 0.1 mol % and conversions between 62 and 90% within 20 h (Table 2, entries 1−4). Under the same conditions, conversion of 1,4-butanediol to γ-butyrolactone is quantitative (entry 5). High conversion of the branched alcohol 1-cyclohexylmethanol (76%) requires slightly higher catalyst loading (0.4 mol %, entry 6). Importantly, no products other than the esters were observed for these reactions; although in the case of 1-heptanol, small amounts of 1-heptanal were also seen, supporting a mechanism with initial aldehyde formation (see above).

Table 2. Iron-Catalyzed Dehydrogenation of Primary Alcohols Using Catalyst 4

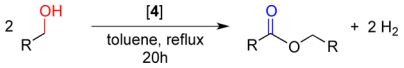

entry	R	catalyst loading	NMR conv. (%)[a]
1	n-C_3H_7	0.1 mol %	90 (75)
2	n-C_4H_9	0.1 mol %	80 (72)
3	n-C_5H_{11}	0.1 mol %	62 (60)
4	n-C_6H_{13}	0.1 mol %	67[b] (62)
5[e]	n-C_3H_6OH	0.1 mol %	99 (85)
6	CH_2-Cy	0.4 mol %	76

[a]Isolated yield in parentheses. [b]2% of 1-heptanal were also detected. [e]Product: γ-butyrolactone.

The reaction mechanism underlying the AAD mediated by bifunctional iron catalyst **4** was further examined using DFT calculations (Scheme 5). We used MeOH and $MeOCH_2OH$ as model substrate and intermediate, respectively, and PMe_2 truncated **4**. Relative free energies reported below have been obtained at the RI-B3PW91-D3BJ/def2-QZVPP//B3LYP/def2-SVP level of density functional theory and refer to the temperature regime employed in the experiments (120 °C). At these conditions, the overall formation of methyl formate is calculated to be slightly endergonic (endothermic) with $\Delta_R G$ = +4.0 kcal mol^{-1} ($\Delta_R H$ = +11.6 kcal mol^{-1}), which is in excellent agreement with experimental data (see the Supporting Information). Starting from the five-coordinate amido complex and methanol (**A1**, Scheme 5), the initial formation of an encounter complex (**A2**) via N···H···O hydrogen bonding is slightly exergonic. From here, concerted O−H/C−H hydrogen transfer from the substrate to the amido species exhibits a moderate barrier (**TS_A2**). It leads to the formation of an encounter complex between formaldehyde and *trans*-dihydride **A3**, which is, however, unbound at ΔG_{393} so that formaldehyde is liberated without barrier, in an exergonic step (**A3** → **A4**). Subsequently, the reaction of formaldehyde with a second equivalent of the substrate to an intermediate hemiacetal (**A5**) occurs in an iron-catalyzed reaction sequence with a small overall reaction barrier (see discussion and Scheme 6 below). Regeneration of the amido complex from the *trans*-dihydride **A5** is a multistep process catalyzed by the substrate (**A6**-**A9**, Scheme 5, bottom): The *trans*-dihydride forms an encounter complex with methanol, featuring simultaneous Fe−H···H−O dihydrogen bonding and N−H···O hydrogen bonding (**A6**), which assists an overall rate-limiting, synchronous proton transfer via **TS_A6** to form dihydrogen complex **A7**. For this step, indirect amine to hydride proton transfer via substrate mediated proton shuttling (Scheme 5) was computed to be slightly favored by $\Delta\Delta G_{393}$ = 3.0 kcal mol^{-1} over direct proton transfer without substrate involvement (see the Supporting Information). At this point we note that rate-limiting H_2 elimination is in line with the observation of **5a** in the stoichiometric reaction of **4** with 1-butanol (see above). Further, such Brønsted-acid catalyzed NH to hydride proton transfer was previously demonstrated experimentally for a related Ru(PNP) hydride complex.[26] The resulting nonclassical dihydrogen complex (**A7**) is stabilized by a hydrogen bond between the basic amide group and MeOH. Elimination of H_2 via **TS_A7** and decoordination of MeOH (**A8**) regenerates the amido complex (**A1**), accompanied by a minute barrier.

Our results discussed so far are in reasonably good agreement with a recent DFT study by Yang focusing on the dehydrogenation of ethanol to acetaldehyde catalyzed by complex **4**.[18] As a consequence of the higher heat of hydrogenation of formaldehyde with respect to acetaldehyde, H_2 transfer from ethanol to **4** was computed to be less endergonic (0.6 kcal mol^{-1}) in this study than we found for our methanol model. Also, Yang reported a stepwise ionic pathway for the alcohol dehydrogenation step, whereas we found a concerted pathway for the dehydrogenation of MeOH. Importantly, however, the barrier for the alcohol-assisted proton shuttling within **5a** represents the highest overall barrier in both studies. Hence, the computed reaction profiles for this branch of overall AAD to ester are relatively robust with respect

dx.doi.org/10.1021/cs5009656 | ACS Catal. 2014, 4, 3994−4003

Scheme 5. Computed Lowest Free-Energy Pathways for Methanol AAD at Catalytic Conditions (120°C) with Model Catalyst [FeH(CO){N(CH$_2$CH$_2$PMe$_2$)$_2$}][a]

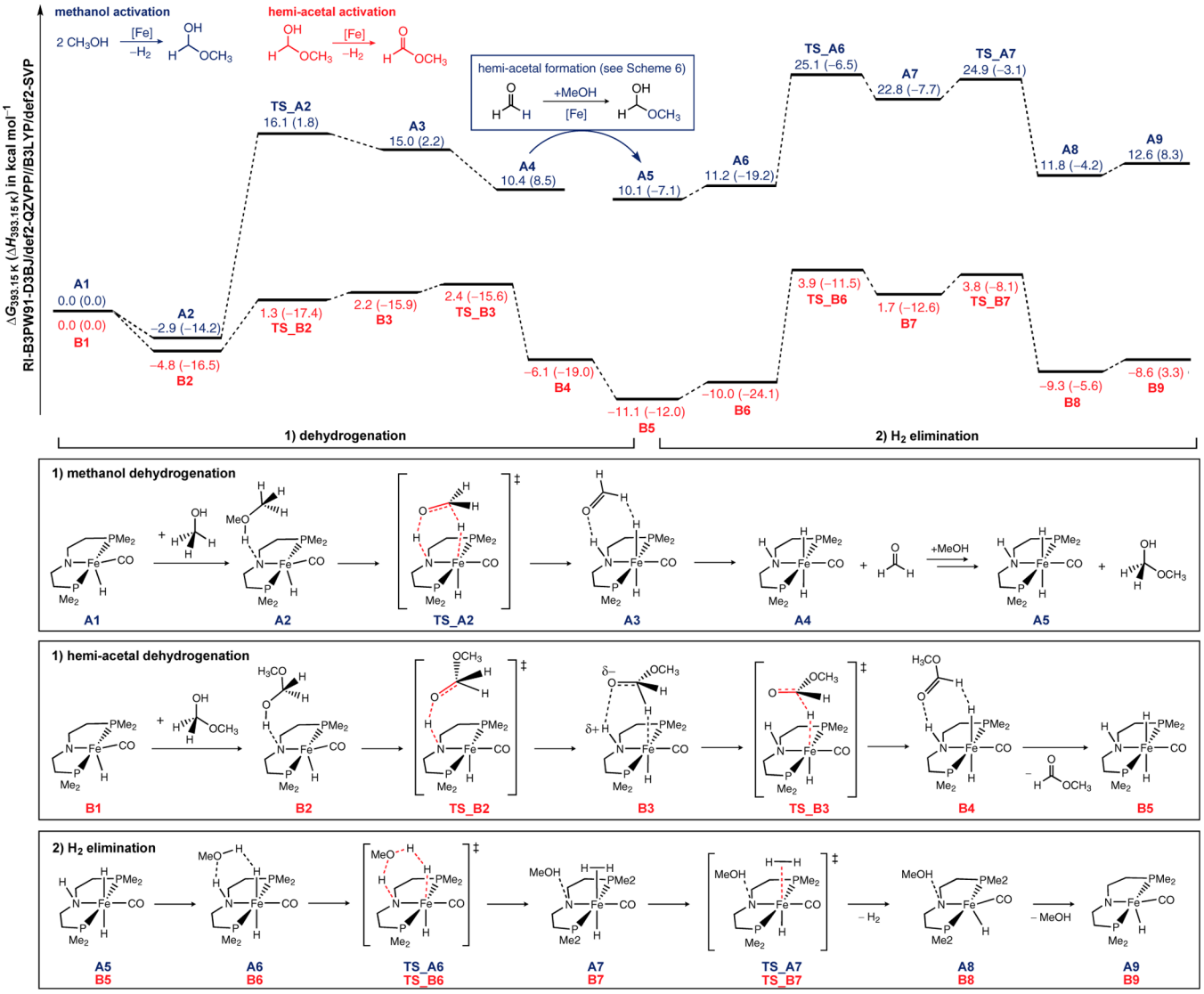

[a]Blue: AAD from H_3COH to H_3COCH_2OH and H_2 (see Scheme 6 for the iron-catalyzed hemiacetal formation through reaction of MeOH with formaldehyde). Red: AAD from H_3COCH_2OH to $H_3COC(O)H$ and H_2. Free energies ΔG and enthalpies ΔH in kcal mol^{-1} computed at the RI-B3PW91-D3BJ/def2-QZVPP//B3LYP/def2-SVP level of DFT.

to the computational methods and to catalyst and substrate truncation, which lends further credibility to these results.

In the second branch of the overall reaction (Scheme 5, red), the hemiacetal formed in the first part of the reaction sequence is further dehydrogenated by the parent amide (**B1**) yet in a slightly different fashion: In contrast to the concerted hydrogen transfer onto the amido catalyst found in the case of MeOH, we did not find a single transition state for a concerted dehydrogenation of the hemiacetal but a stepwise reaction sequence: After formation of the N···H···O hydrogen bridged complex **B2** in a slightly exergonic step, protonation of the amido ligand occurs with a low barrier of 6.1 kcal mol^{-1} (**TS_B2**). Yet, although the resulting complex **B3** is a clearly characterized stationary point identified by intrinsic-reaction-coordinate following calculations running downhill from the preceding transition state based on total energies, it does not represent a stable species on the free energy surface. Hydrogen transfer to the metal center (**TS_B3**) proceeds with a low barrier to give complex **B4**. The latter subsequently decoordinates methyl formate yielding the *trans*-dihydrido intermediate **B5** in an exergonic step, akin to the situation found for the methanol dehydrogenation. The *trans*-dihydrido intermediate then undergoes the same methanol catalyzed H_2 elimination as reported above to close the catalytic cycle (Scheme 5, bottom). Hence, irrespective of some technical differences, both the methanol dehydrogenation (**A2** → **A4**) and the hemiacetal dehydrogenation (**B2** → **B5**) represent single elementary steps in the free energy regime, the former endergonic and the latter exergonic, with effective free-energy barriers of ΔG_{393} = 19.0 kcal mol^{-1} and 7.2 kcal mol^{-1}, respectively, and without occurrence of intermediates.

For the hemiacetal formation step from formaldehyde and methanol sketched in Scheme 5 we investigated three different routes. In line with recent theoretical work of Azofra et al. we compute large activation barriers for the noncatalyzed as well as the methanol-assisted reaction steps (Schemes 6a and 6b).[30]

dx.doi.org/10.1021/cs5009656 | ACS Catal. 2014, 4, 3994−4003

Scheme 6. Computed Free-Energy Pathways for Hemiacetal Formation from Methanol and Formaldehyde: (a) Direct Coupling Step; (b) Methanol Assisted Step; and (c) Iron Catalyzed Path[a]

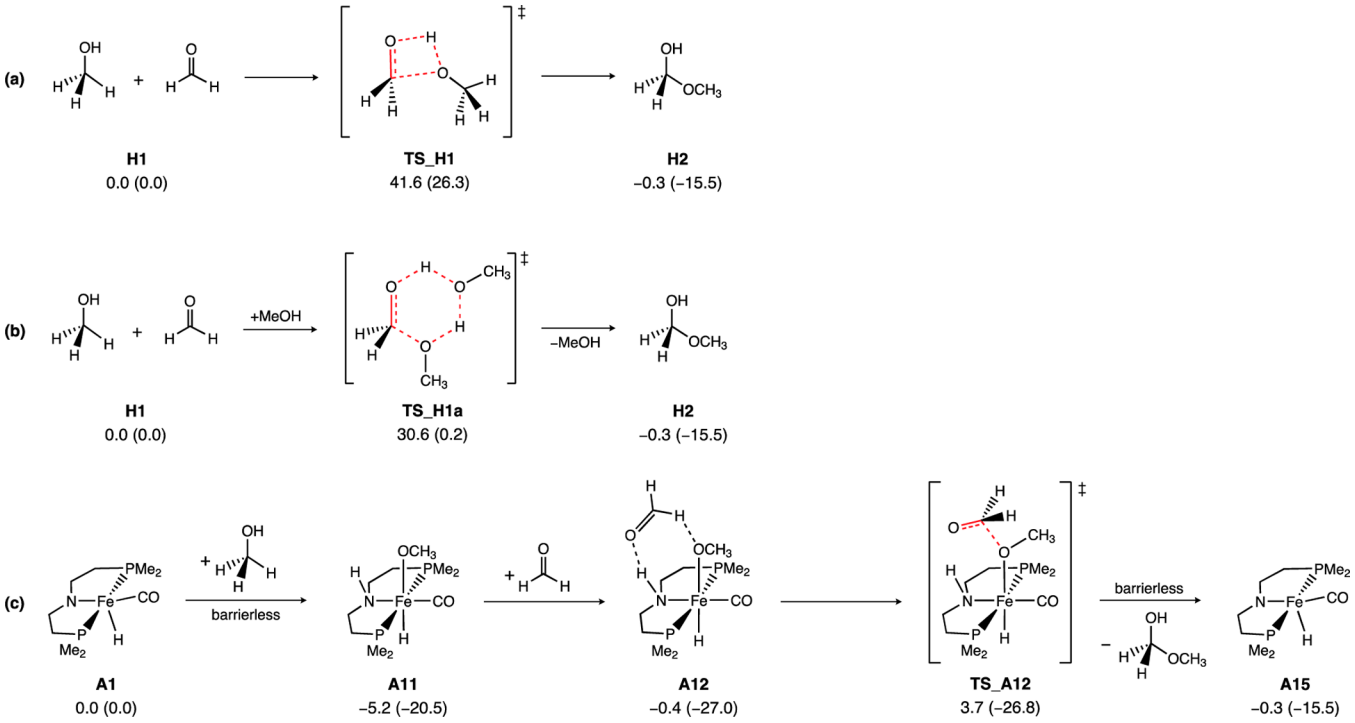

[a]Free energies ΔG and enthalpies ΔH in kcal mol^{-1} computed at the RI-B3PW91-D3BJ/def2-QZVPP//B3LYP/def2-SVP level of DFT.

Table 3. Iron-Catalyzed Hydrogenation of Acetophenones

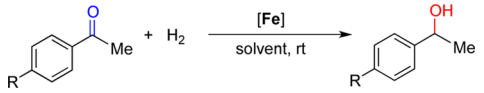

entry	R	catalyst (loading)	p (bar)	solvent	time (h)	T	NMR conv. (%)
1	OMe	**2** (1 mol %)	5.5	toluene	8	r.t.	100
2	OMe	**3** (1 mol %)[a]	5.5	THF	8	r.t.	100
3	OMe	**4** (1 mol %)	5.5	toluene	8	r.t.	100
4	H	**4** (0.2 mol %)	1	THF	2	r.t.	100
5	H	**4** (0.1 mol %)	5	THF	4	r.t.	100
6	H	**4** (0.1 mol %)	5	THF	2	50 °C	100
7	H	**4** (0.05 mol %)	5	THF	4	50 °C	100

[a]10 mol % of KO^{t}Bu with respect to catalyst **3** was used as activator.

We found, however, a low-barrier reaction sequence catalyzed by iron complex **A1** commencing with a barrierless addition of methanol across the Fe−N bond to form **A11** in a moderately exergonic step. Subsequent formation of a loose encounter complex with formaldehyde (**A12**) initiates the C−O coupling step via **TS_A12**, and liberation of the hemiacetal regenerates the catalyst **A15**. Hence, with an overall free-energy barrier of 8.9 kcal mol^{-1}, the hemiacetal formation step is efficiently catalyzed by the iron amido complex (complete presentation of path (c) in the Supporting Information).

Overall, the calculations fully support our initial mechanistic speculations and emphasize the role of metal−ligand cooperativity in the reaction course. Since the AAD reaction of primary alcohols to esters represents the reverse process of ester hydrogenation, as described by Beller and Guan,[15,16] our computational results are also relevant for this reaction.

Ketone hydrogenation, on the other hand, represents the reverse reaction of secondary alcohol dehydrogenation (see above) but has not been previously examined with these Fe(PNP) catalysts. The hydrogenation of carbonyl compounds with bifunctional iron catalysts has been examined in recent years by the groups of Casey, Morris and Milstein.[27] However, some substrates still remain challenging with respect to conversion and/or chemoselectivity.

The model substrate 4′-methoxyacetophenone was hydrogenated (5.5 bar H_2) in toluene in the presence of precatalyst **2** (1 mol %) at room temperature (Table 3, entry 1). Quantitative conversion to 1-(4′-methoxyphenyl)ethanol was achieved within 8 h as determined by NMR spectroscopy. Complex **3** in the presence of KO^{t}Bu (10 mol %) also serves as an equally effective precatalyst (entry 2). Moreover, when the five-coordinate complex **4** was used as the catalyst, similar catalytic activity was observed (entry 3). Further possible

dx.doi.org/10.1021/cs5009656 | ACS Catal. 2014, 4, 3994−4003

reduction of the catalyst loading or pressure is demonstrated for catalyst **4**: Acetophenone is selectively hydrogenated to 1-phenylethanol at room temperature within 2 h using impressively low catalyst loading and H_2 pressure (0.2 mol % **4**, 1 bar H_2, entry 4). The catalyst loading can be further reduced to 0.1 mol % at slightly higher pressure and reaction times (5 bar H_2, r.t., 4 h, entry 5) or temperature (5 bar H_2, 50 °C, 2 h, entry 6) and even down to 0.05 mol % still at mild and practical conditions for full completion (5 bar H_2, 50 °C, 4 h, entry 7), i.e. TON > 2000. Hence, with respect to activity this system is comparable with the best known homogeneous iron catalysts for ketone hydrogenation.[27e,k] A PMe_3 poisoning experiment (10 equiv with respect to **4**) was also carried out for acetophenone hydrogenation (0.1 mol % **4**, 5 bar H_2, 25 °C). Substrate conversion (68%) was slightly reduced, but catalysis was not inhibited as typically observed for other homogeneous iron catalysts.[27j]

However, besides high activity, the chemoselectivity of catalyst **4** is also remarkable. For example, 2-acetylpyridine (eq 3) is converted in quantitative yield to the respective

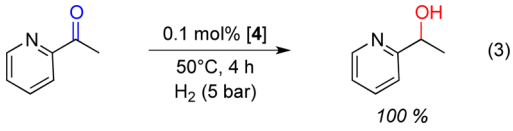

(3)

alcohol with 0.1 mol % **4** at 5 bar H_2 (50 °C, 4 h). In comparison, Milstein's iron catalyst required 15 h (87% yield) under the same conditions,[27e] and Morris' catalyst gave only 20% yield.[27k] As also reported for Morris' catalyst (95% yield),[27k] **4** catalyzes the chemoselective hydrogenation of 5-hexen-2-one to the respective unsaturated alcohol (eq 4),

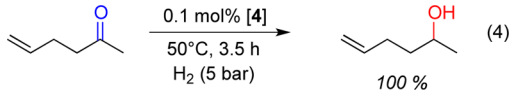

(4)

which provides strong evidence for an outer sphere (bifunctional) mechanism. In addition, **4** exhibits high chemoselectivity with an α,β-unsaturated ketone (eq 5), and only minor

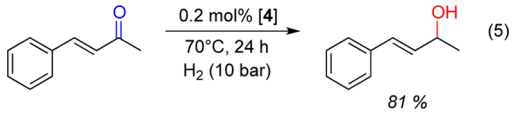

(5)

formation of the respective saturated ketone (12%) and alcohol (2%) is observed. In contrast, Milstein's iron catalyst is not selective with respect to these three products, and Morris' catalyst exhibited no conversion.

In summary, inexpensive homogeneous catalysts using earth-abundant iron have been utilized for the acceptorless dehydrogenation of alcohols and diols and for the reverse hydrogenation of challenging ketone substrates. The yields and chemoselectivities under mild, base free conditions for this system are remarkable compared with previous iron catalysts. Initial mechanistic examinations are in agreement with homogeneous catalysis for de/hydrogenation. The five-coordinate iron amido hydride species **4** is proposed to be the active catalyst in the dehydrogenation reaction, as supported by DFT calculations. Currently, our efforts are focused toward more detailed mechanistic studies of the dehydrogenation and hydrogenation reactions, which will be reported in the future.

EXPERIMENTAL SECTION

General Experimental Information. Unless otherwise noted, all the organometallic compounds were prepared and handled under a nitrogen atmosphere using standard Schlenk and glovebox techniques. Dry and oxygen-free solvents such as THF and pentane were collected from an Innovative Technology PS-MD-6 solvent purification system[28] and used throughout the experiments. Toluene was vacuum distilled from a purple solution of Na and benzophenone and stored over 4 Å molecular sieves. $CDCl_3$ was used without further purification. ^1H and ^{13}C NMR were recorded on a Bruker Avance-400 or Bruker Avance-300 spectrometer. Chemical shift values in ^1H and ^{13}C NMR spectra were referenced internally to the residual solvent resonances. GC-MS spectra were recorded on a Shimadzu QP2010 instrument. Complexes **2**−**4** have been previously reported in the literature.[12−17] All the products isolated from the dehydrogenation and hydrogenation reactions are known compounds.[29]

Catalytic Dehydrogenation of 1-Phenylethanol. In a glovebox, an iron complex (25 μmol), KO^{t}Bu (if required), and 1-phenylethanol (833 μmol or 2.5 mmol) were mixed with 5 mL of solvent in a 50 mL flame-dried Schlenk flask. A condenser was attached to the flask, and the whole setup was brought outside the glovebox. The Schlenk flask containing the homogeneous mixture was then stirred under reflux for 24 h. During the reflux, the solution was continuously bubbled with N_2 (~1 atm), and the liberated H_2 gas was allowed to escape through an outlet port (a needle). After the reaction, the solution was allowed to cool to room temperature, filtered through a short silica gel column, and eluted with THF (10−15 mL). The resulting filtrate was evaporated under vacuum to afford an oily residue. Product identification and conversions were obtained from a ^1H NMR spectrum in $CDCl_3$ (Supporting Information).

Dehydrogenation of 1-phenylethanol (1 mol % catalyst **2**) in the presence of elemental mercury (1.5 g, 7.5 mmol) left the catalytic activity unaffected.

For gas analysis, dehydrogenation of 1-phenylethanol (1 mol % catalyst **2**) was carried out for 10 h, and the gas in the headspace was collected by a gastight syringe. H_2 was detected by GC-analysis as compared to an authentic sample of H_2 (see the Supporting Information). Alternatively, dehydrogenation of 1-phenylethanol (302 μL, 2.5 mmol) with catalyst **2** (10 mg, 25 μmol) in toluene (5 mL) was carried out after connecting the head space to a flask charged with $RhCl(PPh_3)_3$ (23 mg, 25 μmol) and cyclooctene (81 μL, 625 μmol) in THF (5 mL) at 60 °C. After 24 h, 84% of the cyclooctene was converted to cyclooctane, according to GC-MS.

For successive addition experiment, in a glovebox a flame-dried 50 mL Schlenk flask was charged with catalyst **2** (10 mg, 25 μmol), 1-phenylethanol (302 μL, 2.5 mmol), and toluene (5 mL). The solution was stirred under reflux for 24 h under a nitrogen atmosphere, and H_2 was allowed to escape through an outlet port. After 24 h, a second batch of 1-phenylethanol (302 μL, 2.5 mmol) was introduced into the system, and the dehydrogenation reaction was carried out for an additional 24 h. After this time, the solution was allowed to cool to room temperature, filtered through a silica gel column, and eluted with more toluene (10 mL). The resulting filtrate was evaporated under vacuum, and the percentage conversion for the second catalytic run was calculated from the relative ^1H NMR integrations.

dx.doi.org/10.1021/cs5009656 | ACS Catal. 2014, 4, 3994−4003

General Procedure for the Iron-Catalyzed Dehydrogenation of Alcohols (A−P) with Catalyst 2. In a glovebox, a 50 mL flame-dried Schlenk flask was charged with catalyst **2** (10 mg, 25 μmol), an alcohol substrate (2.5 or 25 mmol), and 5 mL of toluene (substrates **A**−**L**) or 5 mL of THF (substrates **M**−**P**). After attaching a condenser to the Schlenk flask, the solution was stirred at 120 °C for a specific time under a constant N_2 flow. A needle was placed through the septum on top of the condenser to remove the liberated H_2 gas. After the reaction, the solution was allowed to cool to room temperature, filtered through a short silica gel column, and eluted with THF. The resulting filtrate was evaporated under vacuum to afford the pure product. ^{1}H and ^{13}C{^{1}H} NMR spectra of the products were recorded in $CDCl_3$ and matched with the chemical shifts reported in the literature. Percentage yields were also calculated for these isolated products.

Catalytic Dehydrogenation of Benzyl Alcohol with Complex 2. In a glovebox, a flame-dried 50 mL Schlenk flask was charged with catalyst **2** (10 mg, 25 μmol), benzyl alcohol (259 μL, 2.5 mmol), and toluene (5 mL). The solution inside the flask was then stirred at 120 °C for 8 h under a constant N_2 flow. H_2 was allowed to escape through an outlet port. After the reaction, the solution was allowed to reach room temperature, filtered through a short silica gel column, and eluted with THF. The resulting filtrate was evaporated under vacuum to afford an oily material. ^{1}H NMR spectrum recorded for this residue in $CDCl_3$ showed quantitative formation of benzyl benzoate. No trace of benzaldehyde was found in the ^{1}H NMR spectrum.

General Procedure for the Catalytic Dehydrogenative Coupling of Alcohols or Diols with Complex 4. A Schlenk flask was charged with **4** (0.005 mmol), alcohol, and toluene (2 mL) in a drybox. The flask was then connected to a Schlenk vacuum line, equipped with a condenser and an oil bubbler. The solution was heated (120 °C) with stirring in an open system under a flow of argon for 20 h. After exposing the flasks to air and cooling, naphthalene was added as an internal standard and analyzed by ^{1}H NMR spectroscopy in $CDCl_3$.

General Procedure for the Iron-Catalyzed Hydrogenation of 4′-Methoxyacetophenone. In a glovebox, a 25 mL stainless steel Parr pressure reactor was loaded with an iron complex (25 μmol), KO^{t}Bu (if required), 4′-methoxyacetophenone (375 mg, 2.5 mmol), and 5 mL of toluene (or THF). The reactor was sealed, flushed with H_2 three times, and finally placed under 80 psig of H_2 pressure. The solution was then stirred at room temperature for 8 h. After the reaction, the solution was filtered through a short silica gel column and eluted with THF. The resulting filtrate was evaporated to dryness to afford the pure hydrogenation product. ^{1}H and ^{13}C{^{1}H} NMR spectra of the product were recorded in $CDCl_3$ and matched with the reported spectra in the literature.

General Procedure for Hydrogenation Studies with Catalyst 4. All of the hydrogenation reactions were performed at constant pressures using a stainless steel 50 mL Parr hydrogenation reactor. The temperature was maintained at 50 or 70 °C using an oil bath. The reactor was flushed several times with hydrogen gas at 5 atm prior to the addition of catalyst and substrate. In a glovebox, a vial was charged with **4** (2 mg, 0.005 mmol) and 5 mL of THF, and a separate vial was charged with substrate (5.128 or 2.564 mmol) and 5 mL of THF. Each solution was then transferred to a syringe equipped with a 12 in. needle and stoppered with a rubber septum. Both syringes were taken out of the glovebox and injected to the prepared Parr reactor against a flow of hydrogen gas. In the case of *trans*-4-phenyl-3-buten-2-one, the gas pressure was adjusted to 10 bar once solutions were injected. Small aliquots of the reaction mixture were sampled from a stainless-steel sampling dip tube attached to the Parr reactor. All samples for gas chromatography (GC) analyses were diluted to a total volume of approximately 1 mL using oxygenated methanol. The conversion of hydrogenated ketones was analyzed by an Agilent Technologies 7890A gas chromatograph equipped with a DB-5MS (30 m × 0.25 mm; film thickness 0.25 μm) with an autoinjector (Agilent 7683B). Hydrogen was used as a mobile phase at a column pressure of 5 psi with a split flow rate of 1 mL/min. The injector temperature was 300 °C, and the FID temperature was 300 °C. One method was used to analyze the substrates; the oven temperature began at 40 °C for 1 min, then 15 °C per minute to 200 °C, and finally 200 °C for 1 min. The retention times for substrates and hydrogenated products are provided in the Supporting Information.

PMe_3 Poisoning Test in the Hydrogenation of Acetophenone with Catalyst 4. In a glovebox, a vial was charged with **4** (5 mg, 0.013 mmol) and 10 mL of THF, a second vial was charged with acetophenone (1553 mg, 12.821 mmol) and 10 mL of THF, and a third vial was charged with PMe_3 (10 mg, 0.119 mmol) and 5 mL of THF. Each solution was then transferred to a syringe equipped with a 12 in. needle and stoppered with a rubber septum. The syringes loaded with catalyst and substrate solutions were taken out of the glovebox and injected to the prepared Parr reactor against a flow of hydrogen gas (25 °C, 5 bar H_2). After 20 min, the syringe with the PMe_3 solution was injected into the Parr reactor under a flow of H_2, and conversion was monitored over time by ^{1}H NMR and GC-FID analysis.

■ ASSOCIATED CONTENT

Ⓢ Supporting Information

Experimental procedures, product characterization data, and details of DFT calculations. This material is available free of charge via the Internet at http://pubs.acs.org.

■ AUTHOR INFORMATION

Corresponding Authors

*E-mail: jones@chem.rochester.edu.

*E-mail: sven.schneider@chemie.uni-goettingen.de.

Author Contributions

⊥These authors (S.C. and P.O.L.) contributed equally.

Notes

The authors declare no competing financial interest.

■ ACKNOWLEDGMENTS

Parts of this work were funded by the Center for Electrocatalysis, Transport Phenomena, and Materials (CETM) for Innovative Energy Storage, an Energy Frontier Research Center funded by the U.S. Department of Energy, and the ESD NYSTAR program (W.D.J.). S.S. and M.C.H. acknowledge support through the COST Action 1205 (CARISMA). P.O.L. is grateful to the Alexander von Humboldt Foundation for a postdoctoral scholarship. N.H. and E.A.B. acknowledge support from the National Science Foundation through the Center for the Capture and Conversion of CO_2 (Grant No. CHE-1240020). Calculations have been performed at the Center for Scientific Computing (CSC) Frankfurt on the FUCHS and LOEWE-CSC high-performance compute clusters.

REFERENCES

(1) (a) Hamid, M. H. S. A.; Slatford, P. A.; Williams, J. M. J. *Adv. Synth. Catal.* **2007**, *349*, 1555−1575. (b) Watson, A. J. A.; Williams, J. M. J. *Science* **2010**, *329*, 635−636. (c) Guillena, G.; J. Ramón, D.; Yus, M. *Chem. Rev.* **2009**, *110*, 1611−1641. (d) Kawahara, R.; Fujita, K.-i.; Yamaguchi, R. *J. Am. Chem. Soc.* **2012**, *134*, 3643−3646. (e) Gunanathan, C.; Milstein, D. *Science* **2013**, *341*, 249.

(2) (a) Junge, H.; Loges, B.; Beller, M. *Chem. Commun.* **2007**, 522−524. (b) Johnson, T. C.; Morris, D. J.; Wills, M. *Chem. Soc. Rev.* **2010**, *39*, 81−88. (c) Nielsen, M.; Kammer, A.; Cozzula, D.; Junge, H.; Gladiali, S.; Beller, M. *Angew. Chem., Int. Ed.* **2011**, *50*, 9593−9597. (d) Trincado, M.; Banerjee, D.; Grützmacher, H. *Energy Environ. Sci.* **2014**, *7*, 2464−2503.

(3) (a) Zhang, J.; Leitus, G.; Ben-David, Y.; Milstein, D. *J. Am. Chem. Soc.* **2005**, *127*, 10840−10841. (b) Gunanathan, C.; Ben-David, Y.; Milstein, D. *Science* **2007**, *317*, 790−792. (c) Patman, R. L.; Williams, V. M.; Bower, J. F.; Krische, M. J. *Angew. Chem., Int. Ed.* **2008**, *47*, 5220−5223. (d) Nixon, T. D.; Whittlesey, M. K.; Williams, J. M. J. *Dalton Trans.* **2009**, 753−762. (e) Andrushko, N.; Andrushko, V.; Roose, P.; Moonen, K.; Börner, A. *ChemCatChem.* **2010**, *2*, 640−643. (f) Gnanaprakasam, B.; Zhang, J.; Milstein, D. *Angew. Chem., Int. Ed.* **2010**, *49*, 1468−1471. (g) Dobereiner, G. E.; Crabtree, R. H. *Chem. Rev.* **2009**, *110*, 681−703. (h) Esteruelas, M. A.; Honczek, N.; Oliván, M.; Oñate, E.; Valencia, M. *Organometallics* **2011**, *30*, 2468−2471. (i) Maggi, A.; Madsen, R. *Organometallics* **2012**, *31*, 451−455. (j) Rigoli, J. W.; Moyer, S. A.; Pearce, S. D.; Schomaker, J. M. *Org. Biomol. Chem.* **2012**, *10*, 1746−1749. (k) Kossoy, E.; Diskin-Posner, Y.; Leitus, G.; Milstein, D. *Adv. Synth. Catal.* **2012**, *354*, 497−504.

(4) For example, the dehydrogenation of isopropyl alcohol to form acetone and H_2 is endothermic by ∼16.5 kcal/mol Wiberg, K. B.; Crocker, L. S.; Morgan, K. M. *J. Am. Chem. Soc.* **1991**, *113*, 3447−3450.

(5) The entropic contribution for a reaction accompanying H_2 liberation at room temperature is ∼8 kcal/mol: Watson, L.; Eisenstein, O. *J. Chem. Educ.* **2002**, *79*, 1269.

(6) For Ru-based catalysts, see: (a) Dobson, A.; S. Robinson, D. *J. Organomet. Chem.* **1975**, *87*, C52−C53. (b) Dobson, A.; Robinson, S. D. *Inorg. Chem.* **1977**, *16*, 137−142. (c) Morton, D.; Cole-Hamilton, D. J. *J. Chem. Soc., Chem. Commun.* **1987**, 248−249. (d) Ligthart, G. B. W. L.; Meijer, R. H.; Donners, M. P. J.; Meuldijk, J.; Vekemans, J. A. J. M.; Hulshof, L. A. *Tetrahedron Lett.* **2003**, *44*, 1507−1509. (e) Jung, C. W.; Garrou, P. E. *Organometallics* **1982**, *1*, 658−666. (f) Zhang, J.; Gandelman, M.; Shimon, L. J. W.; Rozenberg, H.; Milstein, D. *Organometallics* **2004**, *23*, 4026−4033. (g) Junge, H.; Beller, M. *Tetrahedron Lett.* **2005**, *46*, 1031−1034. (h) Adair, G. R. A.; Williams, J. M. J. *Tetrahedron Lett.* **2005**, *46*, 8233−8235. (i) van Buijtenen, J.; Meuldijk, J.; Vekemans, J. A. J. M.; Hulshof, L. A.; Kooijman, H.; Spek, A. L. *Organometallics* **2006**, *25*, 873−881. (j) Hamid, M. H. S. A.; Williams, J. M. J. *Chem. Commun.* **2007**, 725−727. (k) Hollmann, D.; Tillack, A.; Michalik, D.; Jackstell, R.; Beller, M. *Chem.—Asian J.* **2007**, *2*, 403−410. (l) Shahane, S.; Fischmeister, C.; Bruneau, C. *Catal. Sci. Technol.* **2012**, *2*, 1425−1428. (m) Montag, M.; Zhang, J.; Milstein, D. *J. Am. Chem. Soc.* **2012**, *134*, 10325−10328. (n) Tseng, K.-N. T.; Kampf, J. W.; Szymczak, N. K. *Organometallics* **2013**, *32*, 2046−2049. (o) Zeng, G.; Sakaki, S.; Fujita, K.-i.; Sano, H.; Yamaguchi, R. *ACS Catal.* **2014**, *4*, 1010−1020.

(7) For Rh-based catalysts, see: (a) Morton, D.; Cole-Hamilton, D. J. *J. Chem. Soc., Chem. Commun.* **1987**, 248−249. (b) Zweifel, T.; Naubron, J.-V.; Grützmacher, H. *Angew. Chem., Int. Ed.* **2009**, *48*, 559−563.

(8) For Ir-based catalysts, see: (a) Lin, Y.; Ma, D.; Lu, X. *Tetrahedron Lett.* **1987**, *28*, 3115−3118. (b) Morales-Morales, D.; Redón, R.; Wang, Z.; Lee, D. W.; Yung, C.; Magnuson, K.; Jensen, C. M. *Can. J. Chem.* **2001**, *79*, 823−829. (c) Fujita, K.-i.; Tanino, N.; Yamaguchi, R. *Org. Lett.* **2006**, *9*, 109−111. (d) Royer, A. M.; Rauchfuss, T. B.; Wilson, S. R. *Inorg. Chem.* **2007**, *47*, 395−397. (e) Royer, A. M.; Rauchfuss, T. B.; Gray, D. L. *Organometallics* **2010**, *29*, 6763−6768. (f) Musa, S.; Shaposhnikov, I.; Cohen, S.; Gelman, D. *Angew. Chem., Int. Ed.* **2011**, *50*, 3533−3537. (g) Fujita, K.-i.; Yoshida, T.; Imori, Y.; Yamaguchi, R. *Org. Lett.* **2011**, *13*, 2278−2281. (h) Li, H.; Lu, G.; Jiang, J.; Huang, F.; Wang, Z.-X. *Organometallics* **2011**, *30*, 2349−2363. (i) Mena, I.; Casado, M. A.; Polo, V.; García-Orduña, P.; Lahoz, F. J.; Oro, L. A. *Angew. Chem., Int. Ed.* **2012**, *51*, 8259−8263.

(9) Bertoli, M.; Choualeb, A.; Lough, A. J.; Moore, B.; Spasyuk, D.; Gusev, D. G. *Organometallics* **2011**, *30*, 3479−3482.

(10) Zhang, G.; Hanson, S. K. *Org. Lett.* **2013**, *15*, 650−653.

(11) Zhang, G.; Vasudevan, K. V.; Scott, B. L.; Hanson, S. K. *J. Am. Chem. Soc.* **2013**, *135*, 8668−8681.

(12) Alberico, E.; Sponholz, P.; Cordes, C.; Nielsen, M.; Drexler, H.-J.; Baumann, W.; Junge, H.; Beller, M. *Angew. Chem., Int. Ed.* **2013**, *52*, 14162−14166.

(13) Koehne, I.; Schmeier, T. J.; Bielinski, E. A.; Pan, C. J.; Lagaditis, P. O.; Bernskoetter, W. H.; Takase, M. K.; Würtele, C.; Hazari, N.; Schneider, S. *Inorg. Chem.* **2013**, *53*, 2133−2143.

(14) Bielinski, E. A.; Lagaditis, P. O.; Zhang, Y.; Mercado, B. Q.; Würtele, C.; Bernskoetter, W. H.; Hazari, N.; Schneider, S. *J. Am. Chem. Soc.* **2014**, *136*, 10234−10237.

(15) Chakraborty, S.; Dai, H.; Bhattacharya, P.; Fairweather, N. T.; Gibson, M. S.; Krause, J. A.; Guan, H. *J. Am. Chem. Soc.* **2014**, *136*, 7869−7872 Provisional US patent application with a serial number of 61/972927, 2014.

(16) Werkmeister, S.; Junge, K.; Wendt, B.; Alberico, E.; Jiao, H.; Baumann, W.; Junge, H.; Gallou, F.; Beller, M. *Angew. Chem., Int. Ed.* **2014**, *53*, 8722−8726.

(17) Chakraborty, S.; Brennessel, W. W.; Jones, W. D. *J. Am. Chem. Soc.* **2014**, *136*, 8564−8567.

(18) Yang, X. *ACS Catal.* **2013**, *3*, 2684−2688.

(19) Similar dual experiments were performed by Hanson and co-workers. See ref 10.

(20) (a) Widegren, J. A.; Finke, R. G. *J. Mol. Catal. A: Chem.* **2003**, *198*, 317−341. (b) Crabtree, R. H. *Chem. Rev.* **2012**, *112*, 1536−1554. (c) Bedford, R. B.; Betham, M.; Bruce, D. W.; Davis, S. A.; Frost, R. M.; Hird, M. *Chem. Commun.* **2006**, 1398−1400. (d) Rangheard, C.; de Julian Fernandez, C.; Phua, P.-H.; Hoorn, J.; Lefort, L.; de Vries, J. G. *Dalton Trans.* **2010**, *39*, 8464−8471. (e) Sonnenberg, J. F.; Coombs, N.; Dube, P. A.; Morris, R. H. *J. Am. Chem. Soc.* **2012**, *134*, 5893−5899. (f) Sonnenberg, J. F.; Morris, R. H. *Catal. Sci. Technol.* **2014**, *4*, 3426−3438.

(21) (a) Murahashi, S.; Naota, T.; Ito, K.; Maeda, Y.; Taki, H. *J. Org. Chem.* **1987**, *52*, 4319−4327. (b) Lin, Y.; Zhu, X.; Zhou, Y. *J. Organomet. Chem.* **1992**, *429*, 269−274. (c) Coleman, M. G.; Brown, A. N.; Bolton, B. A.; Guan, H. *Adv. Synth. Catal.* **2010**, *352*, 967−970. (d) Endo, Y.; Bäckvall, J.-E. *Chem. − Eur. J.* **2011**, *17*, 12596−12601. (e) Buntara, T.; Noel, S.; Phua, P. H.; Melián-Cabrera, I.; de Vries, J. G.; Heeres, H. J. *Angew. Chem., Int. Ed.* **2011**, *50*, 7083−7087.

(22) (a) Zhao, J.; Hartwig, J. F. *Organometallics* **2005**, *24*, 2441−2446. (b) Muñiz, K. *Angew. Chem., Int. Ed.* **2005**, *44*, 6622−6627. (c) Zhang, J.; Balaraman, E.; Leitus, G.; Milstein, D. *Organometallics* **2011**, *30*, 5716−5724.

(23) Kamitani, M.; Ito, M.; Itazaki, M.; Nakazawa, H. *Chem.Commun.* **2014**, *50*, 7941−7944.

(24) Fe-catalyzed AAD with base as co-catalyst was also recently reported: Song, H.; Kang, B.; Hong, S. H. *ACS Catal.* **2014**, *4*, 2889−2895.

(25) (a) de Graauw, C. F.; Peters, J. A.; van Bekkum, H.; Huskens, J. *Synthesis* **1994**, 1007−1017. (b) Manzini, S.; Urbina-Blanco, C. A.; Nolan, S. P. *Organometallics* **2013**, *32*, 660−664.

(26) Friedrich, A.; Drees, M.; Schmedt auf der Günne, J.; Schneider, S. *J. Am. Chem. Soc.* **2009**, *131*, 17552−17553.

(27) (a) Bullock, R. M. *Science* **2013**, *342*, 1054−1056. (b) Casey, C. P.; Guan, H. *J. Am. Chem. Soc.* **2007**, *129*, 5816−5817. (c) Sui-Seng, C.; Freutel, F.; Lough, A. J.; Morris, R. H. *Angew. Chem., Int. Ed.* **2008**, *47*, 940−943. (d) Mikhailine, A.; Lough, A. J.; Morris, R. H. *J. Am. Chem. Soc.* **2009**, *131*, 1394−1395. (e) Langer, R.; Leitus, G.; Ben-David, Y.; Milstein, D. *Angew. Chem., Int. Ed.* **2011**, *50*, 2120−2124. (f) Sues, P. E.; Lough, A. J.; Morris, R. H. *Organometallics* **2011**, *30*, 4418−4431. (g) Lagaditis, P. O.; Lough, A. J.; Morris, R. H. *J. Am. Chem. Soc.* **2011**, *133*, 9662−9665. (h) Mikhailine, A. A.; Maishan, M.

I.; Morris, R. H. *Org. Lett.* **2012**, *14*, 4638−4641. (i) Langer, R.; Iron, M. A.; Konstantinovski, L.; Diskin-Posner, Y.; Leitus, G.; Ben-David, Y.; Milstein, D. *Chem. − Eur. J.* **2012**, *18*, 7196−7209. (j) Mikhailine, A. A.; Maishan, M. I.; Lough, A. J.; Morris, R. H. *J. Am. Chem. Soc.* **2012**, *134*, 12266−12280. (k) Lagaditis, P. O.; Sues, P. E.; Sonnenberg, J. F.; Wan, K. Y.; Lough, A. J.; Morris, R. H. *J. Am. Chem. Soc.* **2014**, *136*, 1367−1380.

(28) Pangborn, A. B.; Giardello, M. A.; Grubbs, R. H.; Rosen, R. K.; Timmers, F. J. *Organometallics* **1996**, *15*, 1518−1520.

(29) (a) Tamura, Y.; Yakura, T.; Haruta, J.-I.; Kita, Y. *Tetrahedron Lett.* **1985**, *26*, 3837−3840. (b) Kuse, M.; Isobe, M. *Tetrahedron* **2000**, *56*, 2629−2639. (c) Schomaker, J. M.; Travis, B. R.; Borhan, B. *Org. Lett.* **2003**, *5*, 3089−3092. (d) Plietker, B. *J. Org. Chem.* **2004**, *69*, 8287−8296. (e) Murphy, J. A.; Commeureuc, A. G. J.; Snaddon, T. N.; McGuire, T. M.; Khan, T. A.; Hisler, K.; Dewis, M. L.; Carling, R. *Org. Lett.* **2005**, *7*, 1427−1429. (f) Jiang, N.; Ragauskas, A. J. *J. Org. Chem.* **2006**, *71*, 7087−7090. (g) Qian, W.; Jin, E.; Bao, W.; Zhang, Y. *Tetrahedron* **2006**, *62*, 556−562. (h) Fujita, K.-i.; Tanino, N.; Yamaguchi, R. *Org. Lett.* **2007**, *9*, 109−111. (i) Berini, C.; Winkelmann, O. H.; Otten, J.; Vicic, D. A.; Navarro, O. *Chem. − Eur. J.* **2010**, *16*, 6857−6860. (j) Manzini, S.; Urbina-Blanco, C. A.; Nolan, S. P. *Organometallics* **2013**, *32*, 660−664.

(30) Azofra, L. M.; Alkorta, I.; Elguero, J.; Toro-Labbé, A. *J. Phys. Chem. A* **2012**, *116*, 8250−8259.